Modelling microstructure evolution in ATI 718Plus® alloy

Aleksey Reshetov[1,a*], Olga Bylya[1,b], Michal Gzyl[1,c],

Malgorzata Rosochowska[1,d], Paul Blackwell[1,e]

[1]Advanced Forming Research Centre, University of Strathclyde, 85 Inchinnan Drive, Inchinnan, Renfrewshire, PA4 9LJ, UK

[a]aleksey.reshetov@strath.ac.uk, [b]olga.bylya@strath.ac.uk, [c]michal.gzyl@strath.ac.uk,

[d]m.rosochowska@strath.ac.uk, [e]paul.blackwell@strath.ac.uk

Abstract. The present study details the results of finite element analysis (FEA) based predictions for microstructure evolution in ATI 718Plus® alloy during the hot deformation process. A detailed description of models for static grain growth and recrystallisation is provided. The simulated average grain size is compared with those experimentally measured in aerofoil parts after trials. The proposed modified JMAK model has proved to be valid in the main body of the extruded part. The results predicted for the surface are less accurate. The recrystallised grain size on the surface is smaller than in the centre of the part which corresponds to the experimental results and reflects the main trend.

Introduction

ATI 718Plus® alloy is a nickel based superalloy developed by ATI Allvac in 2004 [1]. This alloy has enhanced high temperature capability and thermal stability compared with Inconel 718. At the same time ATI 718Plus® alloy retains good formability and weldability. The alloy is mainly used in gas turbine engine and power turbine applications and potentially can be used as a lower cost replacement for Waspalloy and U720, when those alloys are used in the temperature range of 593 °C – 704 °C [2].

The final mechanical properties of components made from ATI 718Plus® rely on the microstructure that forms during the hot deformation process. The ability for predicting and controlling microstructure during the metal forming operations allows the development of efficient manufacturing processes that produce optimized products with enhanced mechanical properties.

The present paper details the results of finite element analysis (FEA) based predictions for the microstructure evolution in ATI 718Plus® alloy during a hot deformation process. Recrystallisation as well as static grain growth models are described. The simulated average grain size is compared with those experimentally measured in aerofoil parts after the trials.

This study uses a modified JMAK (Johnson-Mehl-Avrami-Kolmogorov) – type model for simulating recrystallisation during the hot extrusion process. The model allows the estimation of volume fraction as well as average grain size of recrystallised material during the deformation process.

JMAK-type models represent a classical approach to simulating the kinetics of recrystallisation [3]. The model was first derived by A. Kolmogorov in 1937 [4] and described the crystallisation of melts. Afterwards, this equation was independently obtained by W.A. Johnson and R.F. Mehl in 1939 [5] and M. Avrami [6] used it to describe the kinetics of phase transformation. The advantage of using these types of models is that the approach is well proven for alloys such as Inconel 718 and Waspalloy. However, these models do not consider the morphology of grains and secondary phases. There are also a number of other limitations. The main disadvantage of this approach is the fact that the history of loading is not taken into account, i.e. history of the recrystallisation; the history of temperature changes; stress history. This study describes further development of JMAK-type

model. In particular, the equations for average grain size were rewritten in incremental form required for FEA modelling, as well as influence of η-phase [7] on the static grain growth and recrystallisation were taken into account.

Experimental procedure

The first two operations (see Fig. 1) of the aerofoil manufacturing process were used to verify the microstructure evolution models. The first operation involved heating ATI 718Plus® billets in the furnace at the temperature of 1080 °C for 15 minutes. It was used to verify the model for static grain growth (GG). To obtain a reference microstructure after this operation, the billet was quenched in water immediately after heating.

The hot extrusion of preforms is the second technological operation in the aerofoil manufacturing process. This operation was used to validate the recrystallisation (RX) model for ATI 718Plus® alloy. The extrusion operation was carried out with high strain rate (the order of 10^2 s^{-1}) on Schuler Multiforge – 3500kN press. It is a direct drive horizontal split die upsetting press with separate servo drive motors providing up to 5000kN grip load and 3500kN upsetting force respectively. High-performance servomotors enable programming of diverse ram speed profiles and stroke sequences.

During the extrusion operation dynamic recrystallisation (DRX) takes place. Once the deformation completed, the metadynamic (MDRX) and static (SRX) recrystallisation, as well as GG, are also possible. From previous experience, DRX is known to be a prevailing mechanism of recrystallisation in this process, so efforts were focused on DRX modelling. It should also be noted that neither the experimental nor the modelling part of the study allows the accurate separation of the MDRX and DRX mechanisms of recrystallisation. Therefore, the RX model presented in this work describes both these phenomena with a focus on the last one. Such approach makes this model even more suitable for the real world industrial applications.

Simulations were performed using DEFORM 3D™ Multiple Operation Ver.11.0.1. The process operations were modelled as follows (see Fig. 1):

1) Heating billet in the furnace;
2) Transfer of billet from the furnace to the extrusion dies; contact effects from billet handling were factored into the simulation;
3) Resting billet on the bottom die before extrusion;
4) Extrusion operation;
5) Chilling / time effects due to part / die contact following extrusion.
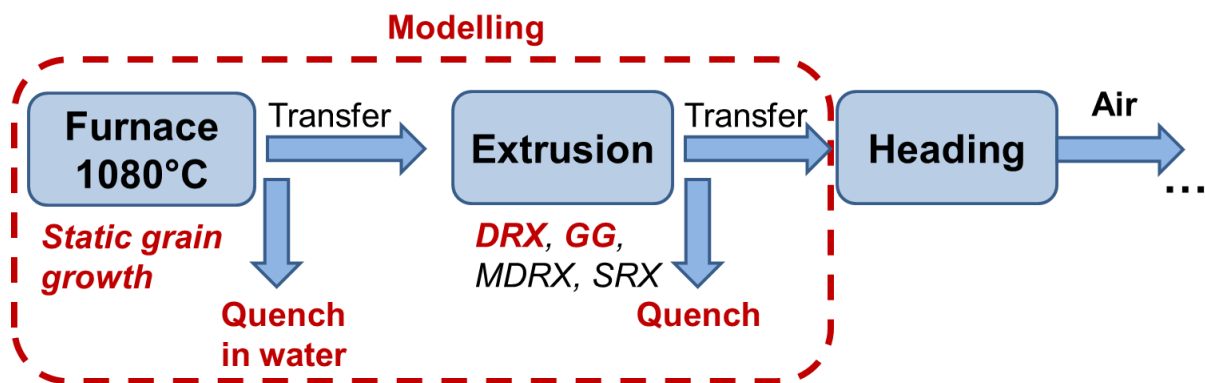

Fig. 1. Manufacturing sequence for obtaining aerofoil preforms from ATI 718Plus® alloy

The work material was modelled as a rigid-plastic, isotropic, Huber-Mises material with flow stress depending on temperature, strain and strain rate. The flow stress data were taken from the ATI 718 Plus® Alloy Data Sourcebook [2] and extrapolated to the higher strain rates of 10^2 s^{-1}. It was also assumed that after a true strain of 1 the alloy behaves like an ideal plastic material. The

friction was described using the Zibel friction law. Thermal properties of ATI 718 Plus[®] were taken from [2]. Convection coefficients were set as a function of temperature based on thermocouple readings obtained during the experimental trials. Contact heat transfer coefficients were defined experimentally and set as a function of applied pressure. The FE model of extrusion was validated by experimental force and velocity readings. The discrepancy between force values obtained in FEA and experiment was within 4%, which implicitly confirms the accuracy of the flow stress data extrapolation.

To obtain a reference microstructure for validation assessment, several extruded billets were quenched immediately after the extrusion operation. Thus, the microstructure immediately following heating and extrusion was fixed for further SEM study.

Microstructure evolution modelling

Static grain growth (GG) model. GG occurs in the initial material during preheating in the furnace. This grain size evolution mechanism can also take place after extrusion, providing that the current temperature is still higher than some threshold value which allows the GG mechanism to be activated. The driving force for this process is the reduction of grain boundary energy through reduction of boundary area.

According to [8], there is no GG in ATI 718Plus[®] alloy below the critical temperature of 975 °C. This temperature is close to the solvus temperature of the η-phase [2] that decorates grain boundaries and impedes grain growth. Thus, this temperature value was set as a temperature threshold for GG activation.

Criteria of activation for static GG:
- Temperature is higher than the critical temperature;
- There is no significant plastic deformation: current strain rate is lower than limiting strain rate (LMTSTR);
- Accumulated (retained) strain is equal to zero (otherwise meta-dynamic or static recrystallisation can be potentially activated).

To simulate the GG, the Eq. 1 [9, 2, 8] was used:

$$D_{gg_i} = \left[D_0^{n_{gg}} + A \cdot t_{eq_i} \cdot \exp\left(-\frac{Q_{gg}}{RT_i} \right) \right]^{1/n_{gg}} \tag{1}$$

where

D_{gg_i} – the average grain size after GG at *i*-step of simulation, [μm];

D_0 – initial grain size, [μm];

T_i – current temperature, [K];

t_{eq_i} – equivalent time for calculating D_{gg_i} with the temperature T_i, [sec];

n_{gg} – the GG exponent;

Q_{gg} – denotes the activation energy for grain growth, [J/mol];

A – material constant;

R – the universal gas constant, [J/(K·mol].

Eq. 1 was incrementally calculated at each time step in FE simulation with user subroutine. Fig. 2 explains the method of defining the average grain size and the equivalent time t_{eq_i} for each step of simulation. The curves T_{i-1}, T_i and T_{i+1} in Fig. 2 schematically represent the rate of grain growth for different heating temperatures.

The equivalent time was calculated for each step according to:

$$t_{eq_i} = t_{D_{i-1}} + \Delta t, \tag{2}$$

where

Δt – time increment of FE simulation, [sec];

$t_{D_{i-1}}$ – time needed to get grain size $D_{gg_{i-1}}$ from the previous step (*i-1*) with temperature T_i at the current step.

Time $t_{D_{i-1}}$ is calculated from Eq. 1 as:

$$ t_{D_{i-1}} = \frac{D_{gg_{i-1}}^{n_{gg}} - D_0^{n_{gg}}}{A \cdot \exp\left(-\dfrac{Q_{gg}}{RT_i}\right)} \tag{3}$$
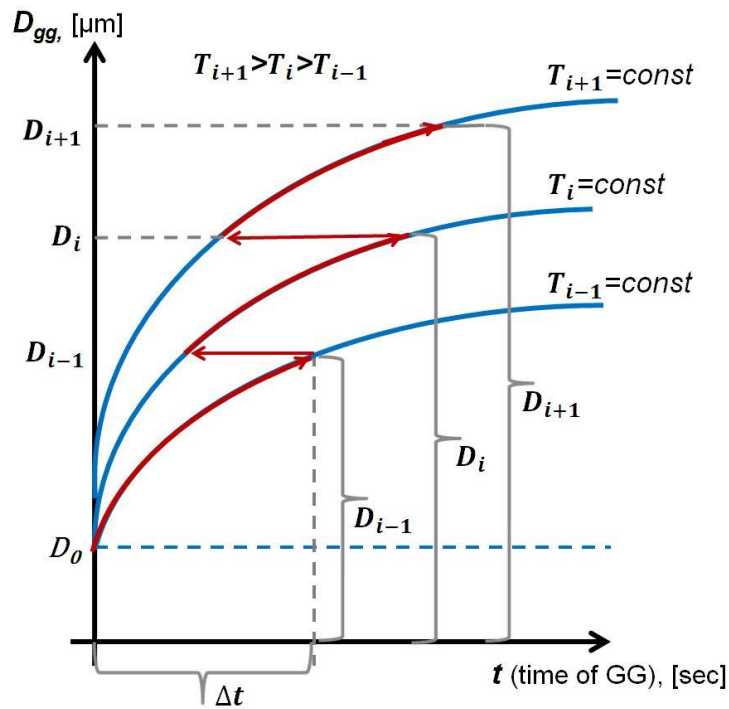

Fig. 2. Computational scheme to calculate average grain size D_{gg} after static grain growth according to Eq. 1

Parameters n_{gg} and A were taken according to the work of Sommitsch *et al* [8]. The activation energy, Q_{gg}, for static GG was taken from the ATI 718Plus® Data Sourcebook [2].

Recrystallisation (RX) model. A modified JMAK (Johnson-Mehl-Avrami-Kolmogorov) – type model adopted from the work of Sommitsch *et al* [8, 10] was employed to simulate the volume fraction of recrystallised (RX) grains in the billet during the hot extrusion operation. The recrystallised fraction was calculated according to equations Eq. 4:

$$ X_{RX} = 1 - \exp\left[\ln(0.5) \cdot \left(\frac{\varepsilon - \varepsilon_{cr}}{\varepsilon_{0.5} - \varepsilon_{cr}} \right)^{m_1} \right], \tag{4}$$

$$ \varepsilon_p = k_p \cdot D_0^{m_3} \cdot Z^{m_4}, $$

$$ \varepsilon_{cr} = k_{cr} \cdot \varepsilon_p, $$

$$ \varepsilon_{0.5} = k_1 \cdot Z^{m_2}, $$

$$Z = \dot{\varepsilon} \cdot \exp\left(\frac{Q}{RT}\right),$$

where:
X_{RX} – recrystallised volume fraction;
ε – accumulated strain at the current step;
ε_p – peak strain (corresponds to flow stress maximum);
$\varepsilon_{0.5}$ – strain needed for 50% recrystallisation;
ε_{cr} – critical strain needed for start of RX;
$\dot{\varepsilon}$ – effective strain rate, [s^{-1}];
Z – Zener-Hollomon parameter;
Q – activation energy for RX, [J/mol];
D_0 – initial grain size, [μm];
T – current temperature, [K];
m_1, m_2, m_3, m_4, k_{cr}, k_p, k_1 – material data.

It should be noted that the parameters k_1, m_1 and m_2 in Eq. 4 are put as semi-temperature dependent - with two different values specified for two temperature ranges: sub-solvus and super-solvus temperatures for the η-phase. By this means, the authors [8, 10] have taken into account the influence of the η-phase on the kinetics of recrystallisation. The parameters for Eq. 4 were defined from the mechanical tests by Sommitsch et al, please refer to the papers [8, 10] for the details.

Due to the complexities in determining the parameters needed for Eq. 4, no attempt was made in this study to distinguish between meta-dynamic or dynamic recrystallisation. Instead of this, it was assumed that the parameter set in Eq. 4 encompasses all possible mechanisms of recrystallisation occurring during/after the deformation process.

The average grain size of new RX grains D_{RX} was calculated based on the accumulated plastic work of deformation according to Eq. 5 [11]:

$$D_{RX} = D_1 + D_2 \cdot \exp\left(-C \cdot \int \bar{\sigma} \cdot \dot{\varepsilon} \cdot dt\right) \tag{5}$$

where:
D_{RX} – average grain size of recrystallised grains, [μm];
D_1, D_2 and C are material constants;
$\bar{\sigma}$ – is current flow stress value, [MPa];
$\dot{\varepsilon}$ – current strain rate, [s^{-1}].

As can be seen from Eq. 5, the RX grain size calculation is based on the accumulated plastic work of deformation, which is usable parameter for FEA simulations due to its stable, integral nature. The main benefit of such an approach is that it takes into account the influence of the loading history. Temperature was accounted for Eq. 5 indirectly through the flow stress function. A more detailed description of the approach is given in [11].

RX activation criteria:
- Current temperature is higher than critical temperature;
- The plastic deformation occurs at the moment: the current strain rate exceeds the limiting strain rate (LMTSTR);
- Accumulated strain is bigger than critical strain ($\varepsilon > \varepsilon_{cr}$).

The models for GG and RX described above were embedded into the DEFORM 3D^{TM} FE package as Fortran user subroutines.

Results and discussion

Fig. 3 shows the results of SEM microstructure study of ATI 718Plus® billet in the as-received condition, as well as after GG in the furnace. As can be seen from Fig. 3a, the initial billet contained η-phase (fine white coloured particles at the grain boundaries). Thus, static grain growth was prevented by Zener pinning until the η-phase solvus temperature was reached. According to the results of experimental grain size measurement, the initial average grain size of about 10 µm has increased to an average grain size of about 70 µm during the heating operation.

The average grain size after 15 minutes of heating in a furnace at the temperature of 1080 °C was calculated using Eq. 1. According to the simulation results, the average grain size increased from the initial value of 10 µm to 62 µm. This grain size is in reasonable agreement with that obtained experimentally (see Fig. 3b).
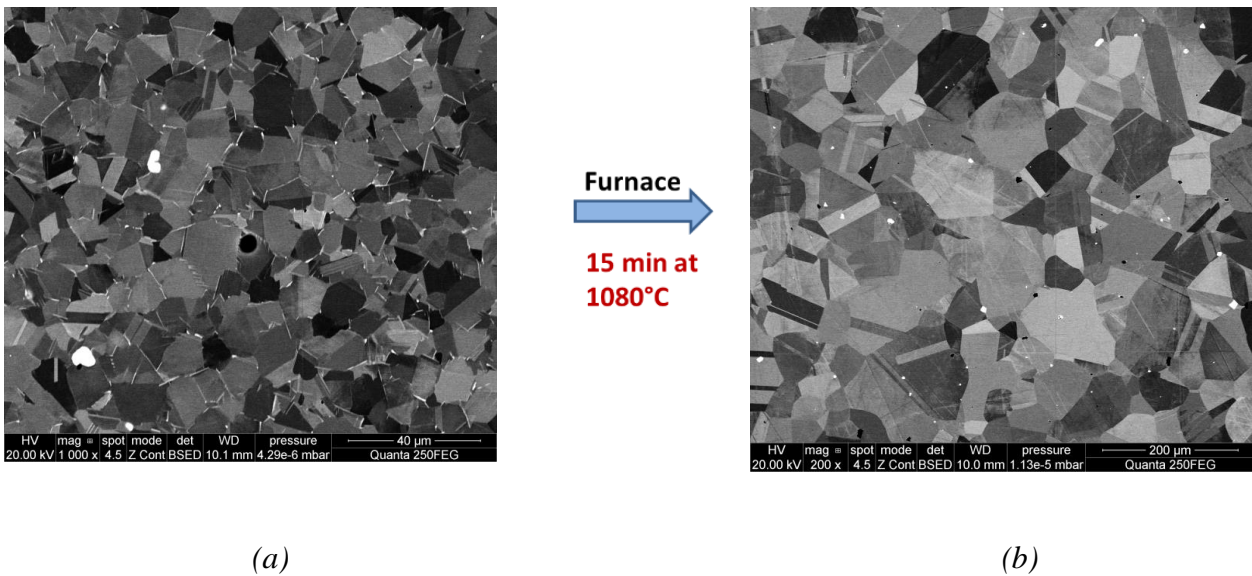

(a)   *(b)*

Fig. 3. SEM microstructure study of ATI 718Plus® billet: (*a*) - Initial material, 10 µm; (*b*) – microstructure after static grain growth in the furnace, 70 µm.

According to the RX simulation results, following extrusion all material in the extruded part was recrystallised (see Fig. 4a). The average RX grain size on the surface of the extrude was calculated to be in the range of 7 – 10 µm (see Fig. 4b). The deep blue colour in Fig. 4b represents a non-extruded and, as a result, non-recrystallised region with the predicted average grain size of 62 µm after static grain growth in the furnace.
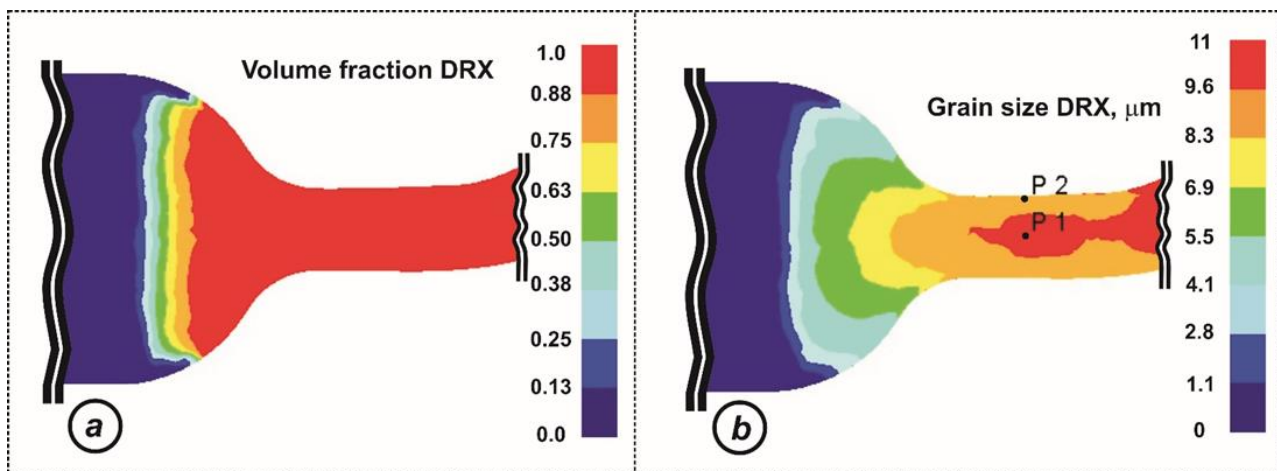

Fig. 4. Results of the base FE simulation with parameters from the experimental trials: (*a*) – volume fraction of recrystallised grains; (*b*) – average grain size of new recrystallised grains

To find out the difference between the grain size in the central and surface region of the extruded cross-section, two reference points were selected (see P1 and P2 in Fig. 4*b*). As can be seen, the grain size in the central part (P1) is 14 μm which is in reasonably good agreement with the experimental results of the microstructure study in this area (10 – 12 μm, see Fig. 5). The grain size on the surface layer is slightly smaller (10 μm for reference point P2 in Fig. 4*b*) than in the central part; this may be linked to cooling during the transfer of the part from the furnace to the forge and the dwell prior to tool closure.

The results of SEM study in the central part of the reference cross-section are shown in Fig. 5. It can be seen that material here looks to be completely recrystallised after extrusion in this area. The average grain size decreased from about 70 μm (see Fig. 3*b*) to 10 – 12 μm (see Fig. 5). The approximate measurements of recrystallised grain size at the surface indicate that the size may be rather smaller – approximately 2 μm. It is difficult to get the precise evaluation of microstructure close to the stem surface due to intensive shear deformation caused by friction. However, it is clear that it is significantly smaller than that predicted by simulation.

It can be concluded that the applied RX model gives good agreement in terms of the average grain size in the centre of the stem cross-section as compared with that obtained experimentally. The RX grain size predicted on the surface is smaller than in the centre which corresponds to the experimental results and reflects the main trend.
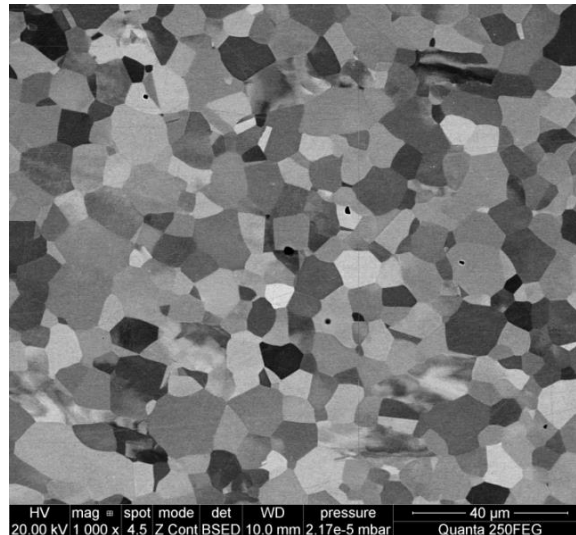

Fig. 5. SEM study of microstructure in the central part of the stem's cross-section after the extrusion operation (grain size: 10 – 12 μm)

Conclusions

The proposed modified model has proved to be valid in the main body of the extruded part. The results predicted for the surface are less accurate. This may be caused by either the model itself or by inaccurate representation of the boundary conditions due to chilling and frictional effects in the contact zone between the workpiece and tools. The question of the adequate representation of these types of boundary conditions in the model needs further consideration. Alongside this, the classical as well as modified JMAK models are limited inasmuch as they disregard information such as the class of grain structure, the precipitate morphology, as well as the history of loading.

The model was developed for the hot extrusion process and is expected to be suitable for a wide range of similar high strain rate forging processes (for strain rates of the order of 10^2 s^{-1}).

The model can be used to assess the influence of selected process parameters on the grain size distribution in ATI 718Plus® parts after hot deformation.

Acknowledgements

References

[1] W.D. Cao, R.L. Kennedy, Role of Chemistry in 718 Type Alloys – Allvac 718Plus Development, Superalloys 2004, TMS (2004) 91-99.

[2] ATI 718 Plus® Alloy Data Sourcebook, ATI Allvac, 2011.

[3] F. Humphreys, M. Hatherly, Recrystallization and related annealing phenomena, Amsterdam: Elsevier (2004), 574.

[4] A. Kolmogorov, Statistical theory of crystallization of metals (in Russian), Bull. Acad. Sci. USSR Ser. Math. 1 (1937) 355–359.

[5] W. Johnson, R. Mehl, Reaction kinetics in processes of nucleation and growth, Trans. Am. Inst. Min. Metall. Eng. 135 (1939) 416–458.

[6] M. Avrami, Kinetics of phase change, I. General theory, The Journal of Chemical Physics, 7 (1939) 1103–1112.

[7] E.J. Pickering, H. Mathur, A. Bhowmik, O.M.D.M. Messe, J.S. Barnard, M.C. Hardy, R. Krakow, K. Loehnert, H.J. Stone, C.M.F. Rae, Grain-boundary precipitation in Allvac 718Plus, Acta Materialia, 60 (2012) 2757–2769.

[8] C. Sommitsch, D. Huber, F. Ingelman-Sundberg, S. Mitsche, M. Stockinger, B. Buchmayr, Recrystallization and grain growth in the nickel-based superalloy Allvac 718Plus, International Journal of Materials Research (formerly Z. Metallkd.). 100 (2009) 1088 – 1098.

[9] P.A. Beck, M.L. Holdsworth, P.R. Sperry, Transactions of the Metallurgical Society of AIME (American Institute of Mining, Metallurgical, and Petroleum Engineers), 180 (1949) 163.

[10] D. Huber, C. Stotter, C. Sommitsch, S. Mitsche, P. Poelt, B. Buchmayr, M. Stockinger, Microstructure modeling of the dynamic recrystallization kinetics during turbine disc forging of the nickel based superalloy Allvac 718Plus[TM], Superalloys 2008, TMS (2008) 855 – 861.

[11] O.I. Bylya, M.K. Sarangi, N.V. Ovchinnikova, R.A. Vasin, E.B. Yakushina, P.L. Blackwell, FEM simulation of microstructure refinement during severe deformation, IOP Conf. Series: Materials Science and Engineering. 63 (2014) doi:10.1088/1757-899X/63/1/012033.